L. Jothi et al. 2019, 7:6
ISSN (Online): 2348-4098
ISSN (Print): 2395-4752

International Journal of Science, Engineering and Technology

An Open Access Journal

Synthesis and Characterization of MnO_2 Nano particles Prepared by Hydrothermal Processing

L. Jothi P.Divya

Department of Physics

Namakkal Kavingnar Ramalingam Government Arts College for Women

Namakkal – 637 001, India, Bishop Heber College, Trichy – 621 017, India

Abstract

In the present project, an attempt has been made to synthesize MnO_2 nanopowders by hydrothermal method at relatively low temperature, short duration and low cost. The amorphous nature of the MnO_2 nano powders were confirmed by using X-Ray diffraction studies. In order to know the functional group present in the MnO_2 nano powders of three different concentration were examined by FTIR spectroscopy in the range of 4000 – 400 cm^{-1}. Optical band gap, absorption spectra and transmittance spectra of three different MnO_2 nanopowders were analyzed using UV - VIS spectroscopy. The surface morphology of the prepared samples were studied. The SEM image of MnO_2 reveals that most of the particles are spherical and few are in nano flakes shape. The elemental analysis and concentration of the nanoparticles in atomic percent has been studied by EDX analysis.

Keywords: Nanopowders, Hydrothermal method, Amorphous nature, Three different concentration.

I. INTRODUCTION

In recent years, passionate research and development input on nanotechnology has delivered nano-objects that possess a rich combination of physical properties, in as much as they differ from those of the bulk and depend on polymorphism, morphology, size of particles, size distribution, coating and the precursor used in the synthesis (1).

With increasing demand for alternative energy sources, electrochemical capacitors with high power densities compared to batteries and high energy density compared to dielectric capacitors are in big demand. They have several advantages like long cycle life, short charge - discharge time and safety. Practical applications are seen for electric vehicles and as memory back up for computers (2). Electrochemical capacitor or super capacitor is a type of storage device that has a high energy density than that of conventional capacitor and a greater power density than those of battery.

Ultrathin porous nanostructures with thicknesses below 10 nm and their three – dimensional self-assembly have been regarded as the goal for the next generation of high performance super capacitors (3). Manganese oxides are one of the considerable importance in technological applications. Manganese oxides including MnO, MnO_2 and MnO_4 are intriguing composites and have been used in waste water treatment, catalysis, sensors, super capacitors and alkaline and rechargeable batteries. Particularly, MnO and MnO_2 nanomaterials have attracted great interest as anode materials (4).

Based on redox reactions between Mn^{2+}, MnO^{4-} and MnO_2 materials have been successfully prepared by hydrothermal method. MnO_2 with various morphologies, such as nanorods and nanowires can be obtained (5). The architectural control of nano and micro-crystals with well defined shapes is an important goal of modern materials science because of the importance shape and texture in determining their varying properties. There are several structure forms of MnO_2 such as α-, β-, γ- and δ-MnO_2, which are made of the basic structure unit [MnO_6] octahedron with different connectivity (6). A large

variety of structural geometries of metal oxide with an electronic structure may exhibit metallic, semiconductor or insulator characteristics endowing them with diverse chemical and physical properties (7). The performance of manganese dioxide in most of these applications could be potentially enhanced by processing one dimensional nanostructure with well-controlled composition, dimensions and morphology (8). Several novel and effective steps have been adopted to prepare manganese oxides nano materials with various shapes and excellent properties such as hydrothermal method (9). In this paper, synthesis and characterization of manganese oxide nano materials with different concentration was investigated.

II. EXPERIMENTAL

The Manganese acetate $Mn(CH_3COO)_2$ of 0.865 g was dissolved in 50 ml of distilled water and stirrer vigorously using magnetic stirrer. Then 0.79 g (1M) Potassium permanganate ($KMnO_4$) in 50 ml of de-ionized water was added. The 2 g of Sodium hydroxide (NaOH) was dissolved in 25ml of water and then added drop wise in above mixture. The entire mixer was stirred vigorously using a magnetic stirrer. After 2 hr of stirring a dark brown colored precipitate of precursor MnO_2 was obtained. The obtained precursor was filtered. The filtered products were dried in hot air oven at 200˚C for 1 hr. After cooling down to room temperature the MnO_2 nanopowder was obtained.

III. RESULTS AND DISCUSSION

1. X-Ray Diffraction Studies

Crystalline phase identification was carried out by X-Ray diffractometer with Cu-Kα radiation (λ=1.54178 Å), the operation voltage and current maintained at 40 kV and 30 mA, respectively. Fig. 1 - 3 shows the XRD pattern of MnO_2 nanoparticles prepared for three different concentrations by hydrothermal method. We see the formation of the crystalline structure. All the diffraction peaks can be readily indexed to a pure tetragonal phase α-MnO_2 with a=9.785 Å and c=2.863 Å. It is difficult to distinguish the MnO_2 phase from the XRD pattern. No characteristic diffraction peaks of manganese oxide species can be detected in the XRD patterns, which could be attributed to the amorphous manganese oxides. Broad diffraction peaks were observed for MnO_2 nano particles, indicating the presence of an amorphous or nano-crystalline phase. Broad peaks were related to a poorly crystallized compound originating from the small grain size and approximately amorphous state of the powder. When amorphous phase is predominant the storage mechanism is likely predominant by only surface adsorption. Therefore, we believe that in such case surface area and pore size could play a key role on the storage properties. Presumably, the MnO_2 appears to be amorphous by XRD because of the small domain sizes, which is not high enough to promote crystallization.

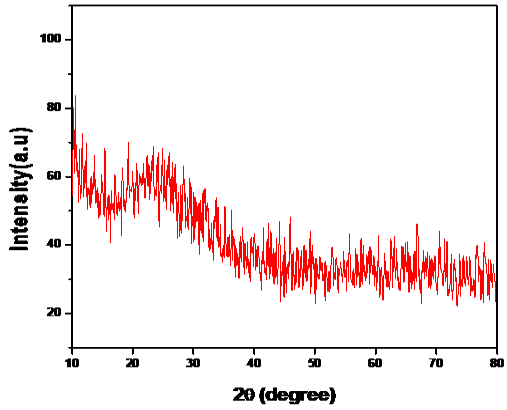

Figure 1: XRD pattern of MnO_2 nanoparticles for 0.1M Concentration of Manganese acetate.

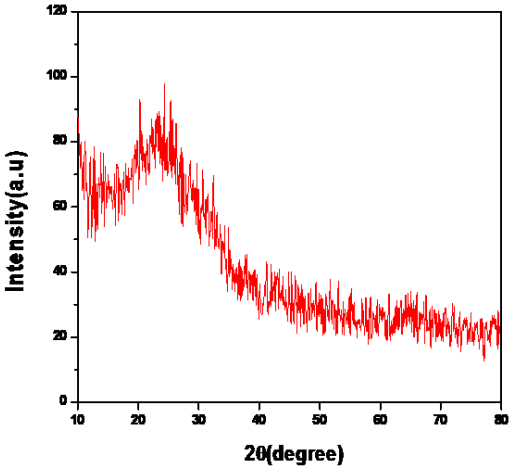

Figure 2: XRD pattern of MnO_2 nanoparticles for 0.15 M concentration of Manganese acetate.

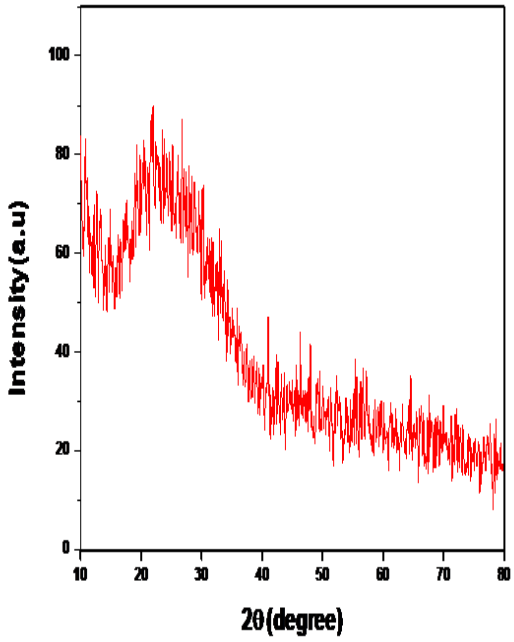

Figure 3: XRD pattern of MnO_2 nanoparticles for 0.2 M Concentration of Manganese acetate.

2. Fourier Transform Infrared Spectroscopy Analysis

In order to know the presence of functional groups synthesized samples, FTIR spectra of MnO_2 nanoparticles different levels were recorded in the range of 4000-400 cm^{-1}. Fig. 4 – 6 shows the FTIR spectrum of MnO_2 nanoparticles for three different concentrations. The absorption peak situated at 516 cm^{-1} corresponds to O-Mn-O characteristic stretching vibration. While the band situated at around 636 cm^{-1} reveals the presence of MnO_6 octahedral, the bands around 2918 and 2994 cm^{-1} correspond to the CH_2 stretching vibrations.

The bands appearing at around 3794 and 1575 cm^{-1} correspond to the O-H stretching and bending vibrations of water molecule adsorbed by the MnO_2. The absorption bands observed around 3714 cm^{-1}, which may be due to the hydrogen-bonded hydroxyl groups, and several small absorption peaks at around 1000-1500 cm^{-1} are attributed to the bending vibrations of O-H bonds. The absorption peak at 516 cm^{-1} can be assigned to Mn-O bending vibrations that arise from MnO_6 octahedron vibration mode.

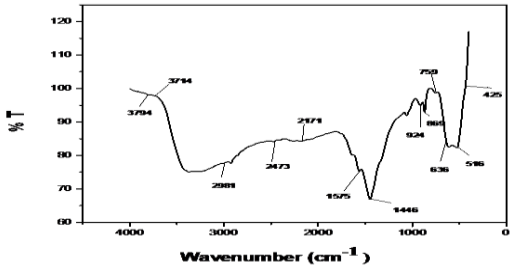

Figure 4: FTIR spectrum of MnO_2 nanoparticles for 0.1 M Concentrations of Manganese acetate.

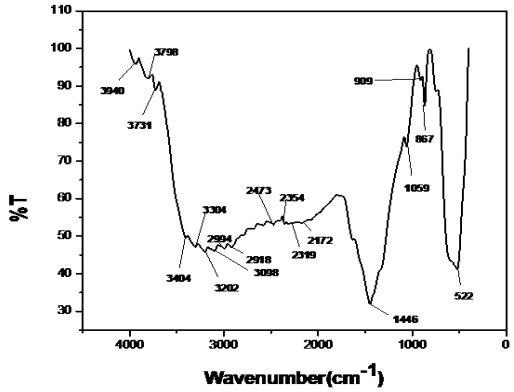

Figure 5: FTIR spectrum of MnO_2 nanoparticles for 0.15 M concentrations of Manganese acetate.

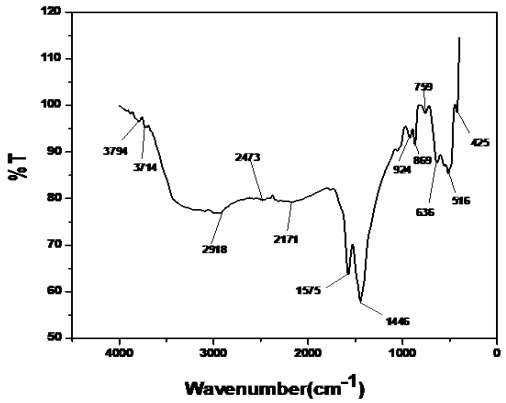

Figure 6: FTIR spectrum of MnO_2 nanoparticles for 0.2 M Concentration of Manganese acetate.

3. Optical Studies Of MnO_2 Nanoparticles

We choose to study the nanoparticles for several reasons. MnO_2 is a technologically important and environmentally friendly wide band gap semiconductor with many unique properties. Several types of devices based on MnO_2 nanocrystals, including field effect transistors, photo detectors and

solar cells have been developed revealing potential applications of MnO_2 nanocrystals for solution-processable electronics.Fig. 7 - 10 shows the normalized UV-Vis absorption spectra of the MnO_2 nanoparticles for three different concentrations. The absorption spectrum of each sample reveals a sharp absorption edge in the UV region and nearly transparent in the visible region. In particular, the energy gap values depend on the films crystal structure, the arrangement and distribution of atoms in the crystal lattice also it is influenced by crystal regularity. The band gap of the film was calculated using the Tauc relationship.

$$\alpha h\upsilon = A(h\upsilon - Eg)^n$$

Where, α is the absorption coefficient, A is the constant, h is the Planck's constant, υ is the photon frequency, Eg is the optical band gap and n is 2 for indirect band gap semiconductors. The functional relationship between $(\alpha h\upsilon)^2$ and photon energy (hυ) for MnO_2 nanoparticles for three different concentrations is shown in Fig. 11 – 13. Since Eg = hυ when $(\alpha h\upsilon)^2 = 0$, an extrapolation of the linear region of the plot of (hυ) versus photo energy on the x-axis gives the value of the optical band gap Eg.

The optical band gap energy of the nanoparticles strongly depends upon the solution concentration. The band gap energy of the MnO_2 nanoparticles increased from 5.84 to 5.93 eV as the MnO_2 concentration increased from 0.1 to 0.2 M. The wider band gap energy for the nanoparticles prepared with 0.2 M can be explained by the Burstein–Moss effect, which is attributed to the transition energy in degenerate semiconductors due to partially filled conduction band.

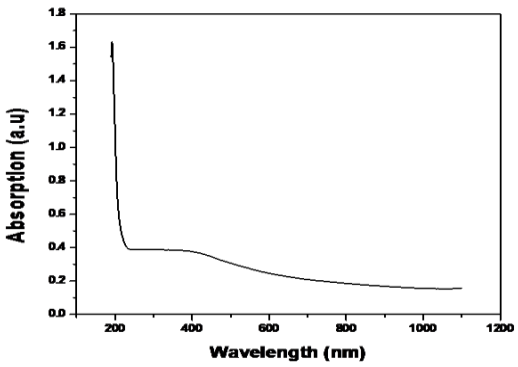

Figure 7: Optical absorption spectra of MnO_2 nanoparticles for 0.1 M concentration of Manganese acetate.

Fig. 13 - 15 shows the normalized UV-Vis transmittance spectra of the MnO_2 nanoparticles for three different concentrations. The transmittance increased in the region of 300-700 nm, when the concentration of Manganese acetate increased from 0.1 to 0.2 M. That is the transmittance increases in the visible and near infrared region with Mn incorporation. All the MnO_2 nanoparticles show an average transmittance greater than 70% in the visible region, indicating good quality of the nanoparticles with low scattering or absorption loses.

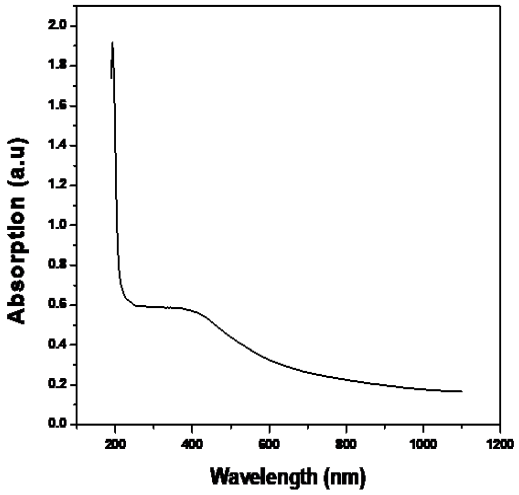

Figure 8: Optical absorption spectra of MnO_2 nanoparticles for 0.15 M concentration of Manganese acetate.

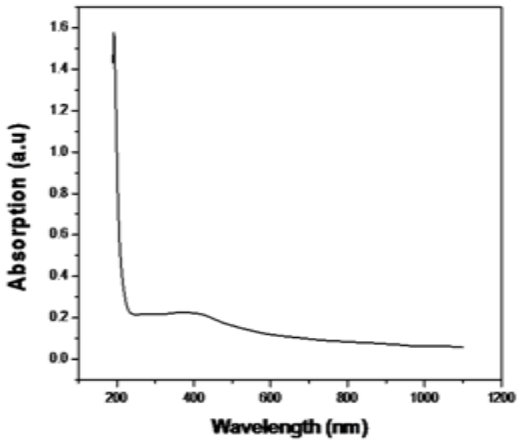

Figure 9: Optical absorption spectra of MnO_2 nanoparticles for 0.2 M concentration of Manganese acetate.

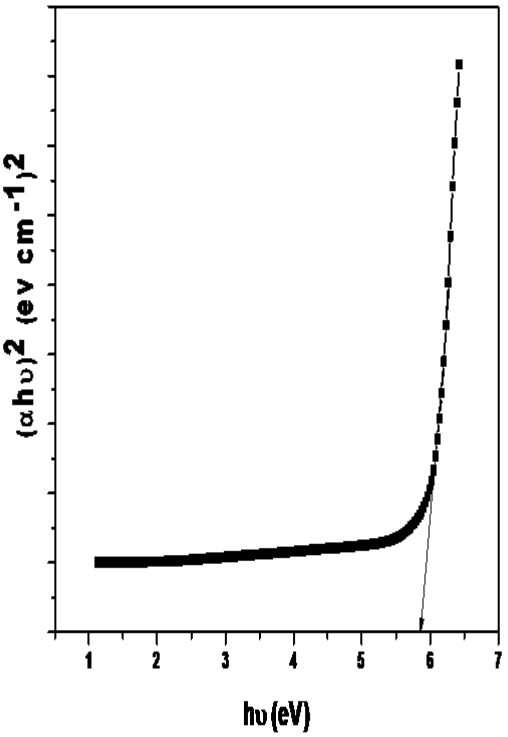

Figure 10: Optical band gap of MnO_2 nanoparticles for 0.1 M concentration of manganese acetate.

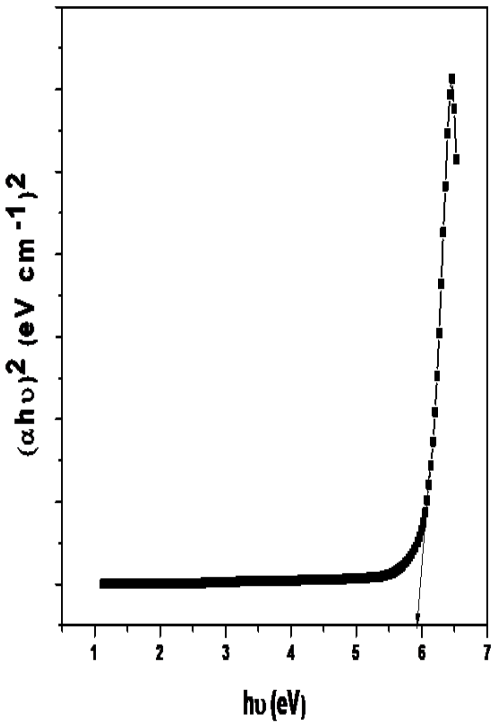

Figure 12: Optical band gap of MnO_2 nanoparticles for 0.2 M concentration of Manganese acetate.

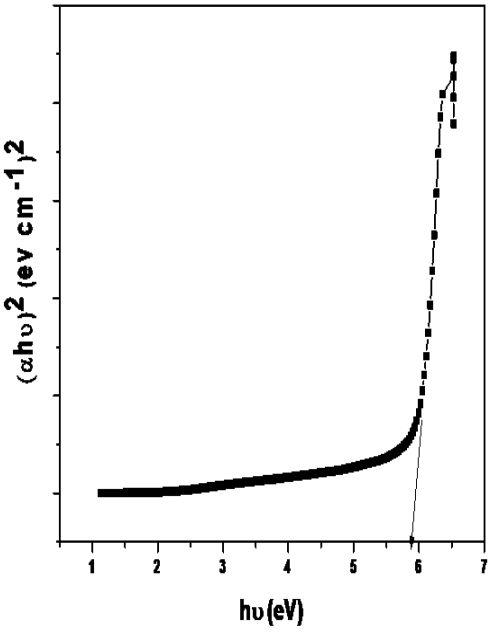

Figure 11: Optical band gap of MnO_2 nanoparticles for 0.15 M concentration of Manganese acetate.

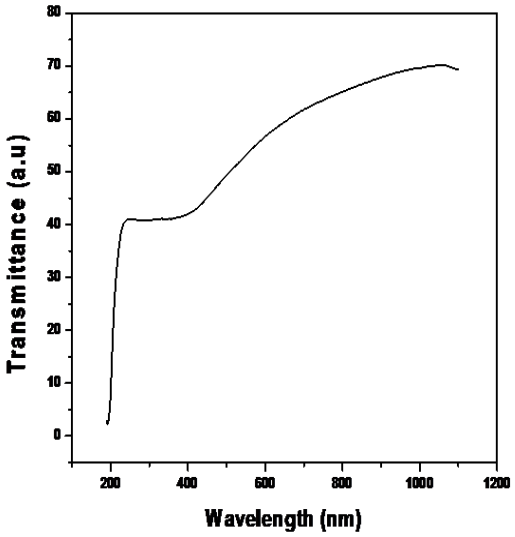

Figure 13: Optical transmittance spectra of MnO_2 nanoparticles for 0.1 M concentration of Manganese acetate.

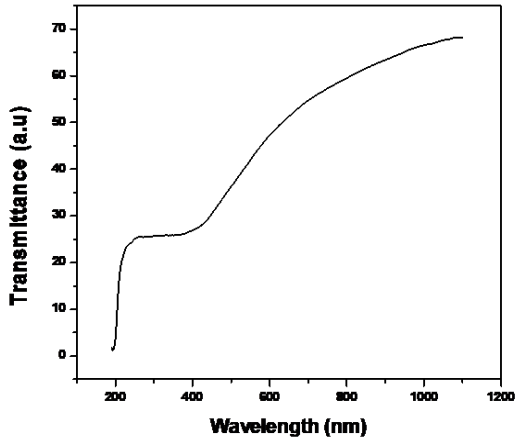

Figure 14:. Optical transmittance spectra of MnO_2 nanoparticles for 0.15 M concentration of Manganese acetate.

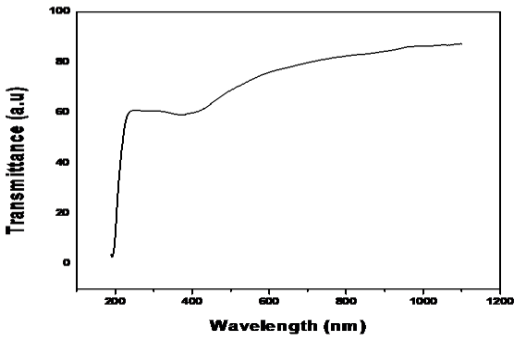

Figure 15: Optical transmittance spectra of MnO_2 nanoparticles for 0.2 M concentration of Manganese acetate.

4. Surface Morphological Studies

The surface morphology of MnO_2 nanoparticles for three different manganese acetate concentrations is shown in Fig. 16-18. This observation suggests uniform MnO_2 nanopowders. The surface morphology of MnO_2 nanopowder shows a porous and rough structure with sponge like morphology. This porous morphology facilitates the diffusion of electrolytes and improves ionic conductivity. Besides, it reduces electrode resistance and accelerates faradic surface reaction feasible for super capacitor applications.

The SEM image of MnO_2 reveals that most of the particles are spherical and few are in nano flakes shape. The sizes of the particles are in the range of 25-30 nm. However, the MnO_2 depicts the completely spherical morphology with the sizes of the particles in the range of 15-20 nm. This indicates the effect of controlling the size and shape of the MnO_2.

Fig. 16-18 shows FESEM images of the synthesized nanoparticle at different MnO_2 concentrations. The morphology of the MnO_2 is flakes like nanoparticles with diameters of 1-2 μm and thickness of 10-20 nm. When the MnO_2 concentration is increased to 0.2 M, the morphology of MnO_2-0.2 M is totally different from that of MnO_2-0.1 M concentrations. It can be seen that the sample consists of urchin like MnO_2 microsphere. Finally, nanoflakes disappeared completely, and all of them assembled into irregular micro-spherical aggregates as shown in Fig. 4 (c).

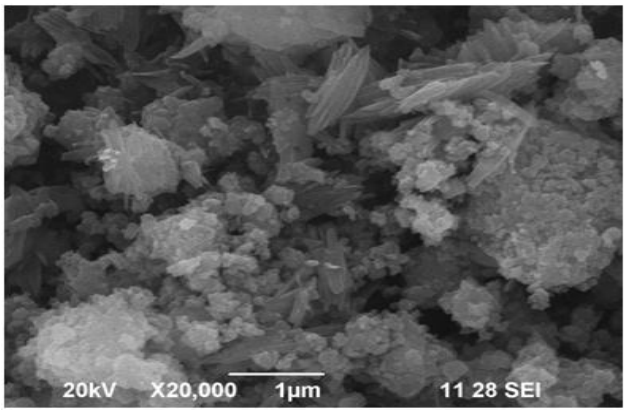

Figure 16: SEM image of MnO_2 nanoparticles for 0.1 M concentration of Manganese acetate.

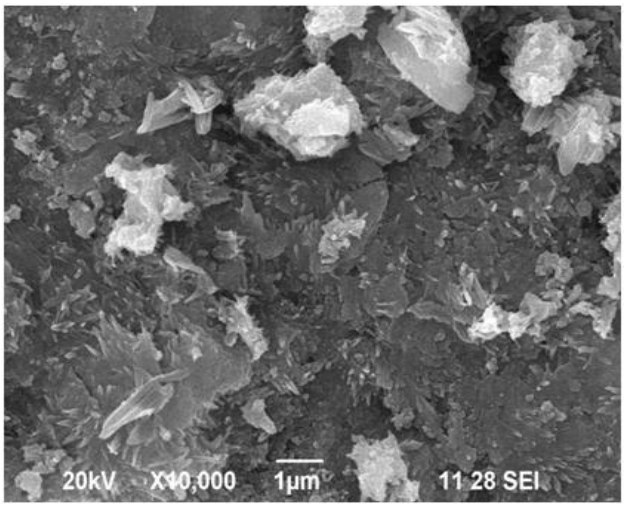

Figure 17: SEM image of MnO_2 nanoparticles for 0.15 M concentration of Manganese acetate.

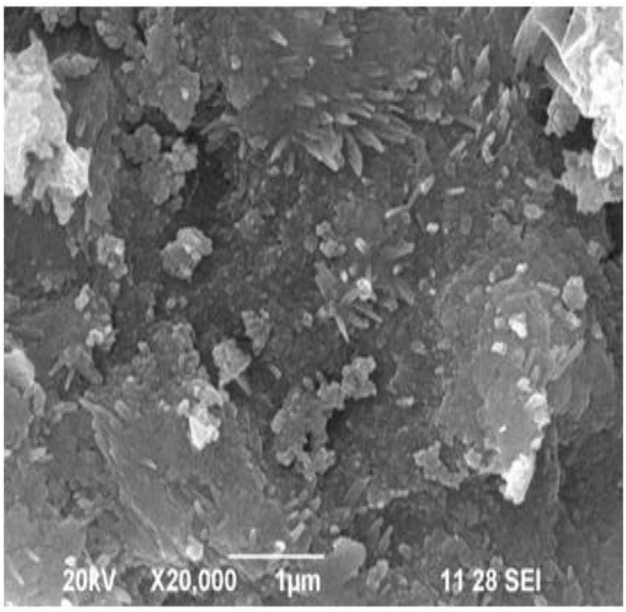

Figure 18: SEM image of MnO_2 nanoparticles for 0.2 M concentration of Manganese acetate.

IV. CONCLUSION

MnO_2 nanoparticles have been synthesized by hydrothermal method. The hydrothermal method is found to be a convenient method for preparation of MnO_2 nanoparticles. The effects of MnO_2 on the structural, optical and morphological properties of the synthesized powders were discussed. XRD pattern of MnO_2 nanoparticles were prepared for three different concentrations. Broad diffraction peaks were observed for MnO_2 nanoparticles indicating the presence of an amorphous or nano-crystalline phase.

FTIR spectrum of MnO_2 nanoparticles of different concentrations confirms that absorption peak at 516 cm^{-1} corresponds to O-Mn-O characteristic stretching vibration. While the band at 636 cm^{-1} reveals the presence of MnO_6 octahedral, the bands around 2918 and 2994 cm^{-1} correspond to the CH_2 stretching vibrations. The absorption spectrum of each sample reveals a sharp absorption edge in the UV region and nearly transparent in the visible region. The band gap energy of the MnO_2 nanoparticles increased from 5.84 to 5.93 eV as the MnO_2 concentration increased from 0.1 to 0.2 M. The wider band gap energy for the nanoparticles prepared with 0.2 M can be explained by the Burstein–Moss effect. All the MnO_2 nanoparticles show an average transmittance greater than 70% in the visible region, indicating good quality of the deposited films with low scattering or absorption loses. The SEM image of MnO_2 reveals that most of the particles are spherical and few are in nano flakes shape. The sizes of the particles are in the range of 25-30 nm. However, the MnO_2 depicts the completely spherical morphology with the sizes of the particles in the range of 15-20 nm. This indicates the effect of controlling the size and shape of the MnO_2.

REFERENCES

[1]. Julien, C.M, Mauger. A, Vijh. A, Zaghib. K. (2006). Lithium Batteries. Science and Technology, 29-68.

[2]. K. Karthikeyan, D. Kalpana, N. G. Renganathan. (2008). Synthesis and characterization of $ZnCo_2O_4$ nanomaterial for symmetric supercapacitor applications. Ionics, 15, 107-110.

[3]. Xiong Zhang, Peng Yu, Haitao Zhang, Dacheng Zhong Sun, Yenwei Ma. (2013). Rapid hydrothermal synthesis of hierarchical nanostructures assembled from ultrathin birnessite-type MnO_2 nanosheets for supercapacitor applications. Electrochimica Acta, 89, 523-529.

[4]. M. Balamurugan, G. Venkatesan, S. Ramachandran and S. Saravanan. (2013). Synthesis and Characterization of Manganese Oxide Nanoparticle, Synthesis and Fabrication of Nanomaterials, 311-314.

[5]. Rongrong Jiang, Tao Huang, Jiali Liu, Jihua Zhuang, Aishui Yu. (2009). A novel method to prepare nanostructure manganese dioxide and its electrochemical properties as a supercapacitor electrode. Elecrochimica Acta, 54, 3047-3052.

[6]. Xiaochan Duan, Jiaqin Yang, Haiyan Gao, Jianmin Ma, Lifang Jiao and Wenjun Zheng. (2012). Controllable hydrothermal synthesis of manganese dioxide nanostructures: shape evalution, growth mechanism and electrochemical properties. Cryst Eng Comm, 14, 4196 – 4204.

[7]. Kanjwal MA, Baralat NAM, Sheikh FA, Khil MS, Kim HY. (2008). Physiochemical Characterization of nanobelts consisting of three mixed oxides (CO_3O_4, CuO and MnO_2) prepared by electro spinning technique. J Mater Sci, 43, 5489-5494.

[8]. Riri Han, Shentao Xing, Zichuan Ma, Yinsu Wu, Yuanzhe Gao. (2012). Effect of the KMnO4 concentration on the structure and

electrochemical behavior of MnO_2. J Mater Sci, 47, 3822 - 3827.

[9]. Xiaodi Liu, Chang Zhong Chen, Xiyang Zhao and Bin Jia. (2013). A Review on the Synthesis of Manganese Oxide Nanomaterials and Their Applications on Lithium-Ion Batteries. Journal of Nanomaterials, 736375, 1-7.